Analysis of the Coupled-bunch Instability for Arbitrary Multibunch Configurations with Application to the NSLS-II Storage Ring

G. Bassi*, A. Blednykh and V. Smaluk

Brookhaven National Laboratory
Upton, NY 11973, USA
**E-mail: gbassi@bnl.gov*

The coupled-bunch instability driven by the resistive wall impedance is studied for multibunch configurations with a gap in the uniform filling. Measurements of the instability thresholds performed at the NSLS-II storage ring are compared with the predictions of a general theoretical eigenanalysis based on the known formulas of the complex frequency shifts for the uniform multibunch configuration case.

Keywords: Coupled-bunch; Instability; Arbitrary Configurations; Resistive Wall

1. Introduction

The design of modern storage rings, with their goal to accumulate high average beam currents, requires detailed studies to minimize detrimental effects on the beam quality driven by short- and long-range wakefields, produced by the electromagnetic interaction of the circulating beam with the storage ring components. The aferomentioned studies do not prevent, however, plans for operation above the wakefields driven instability current thresholds. Multibunch operations, for example, above threshold is made possible by the use of feedback systems, and the determination of the most stable multibunch configuration is of crucial importance for their efficient use, especially in cases where the multibunch filling pattern deviates significantly from the uniform one.

In this contribution we discuss measurements of the coupled-bunch instability driven by the resistive wall impedance in the NSLS-II storage ring. The measurements of the instability thresholds, performed with a varying gap in the uniform filling, are compared with the theoretical predictions of the eigenanalysis developed in[1], where it is shown that the coupled-bunch instability threshold for an arbitrary filling pattern is determined by the solution of an eigenvalue problem based on the known formulas of the complex frequency shifts for the uniform filling pattern case.

2. Resitive Wall Impedance Budget of NSLS-II

For the resistive wall impedance of one component of the storage ring we use the standard thick wall formula[a]

$$Z_1^{\perp}(\omega) = (1 - i\mathrm{sgn}(\omega))\frac{Z_0 s_0 L\sqrt{s_0 c|\omega|}}{2\pi\omega b^4}, \quad s_0 = \Big(\frac{2b^2}{Z_0\sigma_c}\Big)^{1/3}, \quad (|\omega| \le c/s_0). \qquad (1)$$

where Z_0 is the impedance of free space and c the speed of light, and where L, $\sigma_{\rm c}$ and b are the length, conductivity and half aperture of the impedance structure respectively. The conductivities of the material of the storage ring components are shown in Table 1, and the relevant contributions to the vertical resistive wall impedance budget are shown in Table 2, where a distinction is made between contributions from arcs and straigth sections. In Table 2 the different elements have the following meaning: chamber (CH), fast corrector (FC), in-vacuum undulator (IVU), damping wiggler (DW). The contribution from N elements, each of length

Table 1. Thermal conductivity of resistive wall components

Material	Symbol	σ_c(MS/m)
Stainless steel	SS	1.35
Alluminum	Al	31.6
Copper	Cu	54
Non-Evaporable Getter	NEG	2
Inconel	Inc	0.775
Titanium	Ti	1.67

L_i, is weighted by

$$\bar{\beta}_{y,i} = \Big[\frac{1}{L_i}\int_{s_i-L_i/2}^{s_i+L_i/2}\frac{ds'}{\beta_y(s')}\Big]^{-1}, \qquad i = 1, \cdots, N, \qquad (2)$$

where s_i is the ring location of the center of the element. Eq.(2) reduces to the standard relation $\bar{\beta}_{y,C} = C/(2\pi\nu_y)$ for a global impedance distributed along the ring circumference C.

Eliminating s_0 in Eq.(1), we notice that ${Z_1}^{\perp}$ can be rewritten in the form

$$Z_1^{\perp}(\omega) = (1 - i\mathrm{sgn}(\omega))\frac{\sqrt{2Z_0 c|\omega|}}{2\pi\omega}\frac{L}{\sqrt{\sigma_c}b^3}. \qquad (3)$$

We thus define the total average impedance $\bar{Z}_1^{\perp}$ as

$$\bar{Z}_1^{\perp}(\omega) = (1 - i\mathrm{sgn}(\omega))\frac{\sqrt{2Z_0 c|\omega|}}{2\pi\omega}K, \qquad (4)$$

[a]The use of Eq.1 is justified by the thickness of the storage ring components and by the fact that the lowest frequency contribution to the coupled-bunch instability threshold is given by $\mathrm{Re}Z_{\perp}$ sampled at $(1-q)\omega_0$, where ω_0 is the angular revolution frequency and q the fractional part of the betatron tune $\nu_\beta = \omega_\beta/\omega_0$, where ω_β is the betatron frequency.

where

$$K = \sum_i \alpha_i, \quad \alpha_i = \frac{\bar{\beta}_{y,i}}{\sqrt{\sigma_{c,i}}\bar{\beta}_{y,C} b_i^3}. \tag{5}$$

The last column of Table 2 shows the contributions in percentage of the relevant impedance elements, contributing to 90% of the vertical resistive wall impedance budget. Fig.1 shows the beta functions of two cells of the NSLS-II storage ring[2], which adopts a DBA lattice with 30 periods, thus dividing the storage ring in 30 cells. The two cells shown in Fig.1 correspond to one super-period of the lattice.

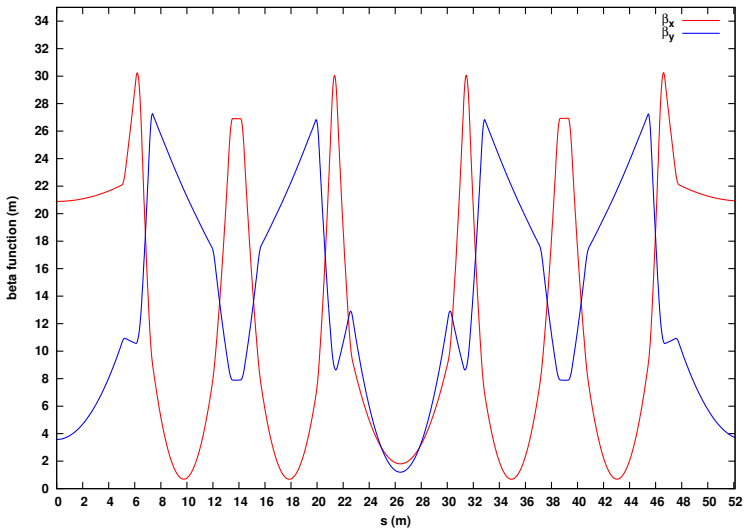

Fig. 1. One superperiod of the NSLS-II DBA lattice consisting of two cells with short and long straigth sections.

3. Coupled-bunch Instability for Arbitrary Fillings

The coupled-bunch instability for arbitrary filling patterns has been discussed in the literature with various degrees of approximation[3,4,5]. In this contribution we apply the general analysis developed in[1], where starting from a system of $M-$coupled Vlasov equations governing the evolution of the phase space densities Ψ_m associated with the m-th bunch $(m = 0, ..., M-1)$, it is shown that the stability analysis is reduced to the formulation of an eigenvalue problem defined by the complex frequency shifts of the uniform filling pattern case. The numerical solution of the eigenvalue problem, via the calculation of the eigenvalue with the largest growth rate (largest imaginary part), allows the determination of the coupled-bunch instability threshold by equating the fastest growth time to the radiation damping time.

Table 2. Main contributions to the vertical resistive wall impedance.

Contribution from arcs:						
	Element	Material	L(m)	$\bar{\beta}_y$(m)	b(mm)	α/K(%)
	CH1	Al	536.4	7.8	12.5	35
	CH2	SS	11.5	7.8	12.5	3.6
	FC	Inc	5.8	7.8	12.5	2.4
Contribution from straight sections:						
Cell	Element	Material	L(m)	$\bar{\beta}_y$(m)	b(mm)	α/K(%)
1[a]	CH	Al	5.36	7	12.5	2.2[a]
1[b]	FC	Inc	0.37	8.3	12.5	4.9[b]
3	IVU	Cu	4.2	2.5	3.2	4.0
4	IVU	Cu	3.46	3.8	3.4	4.2
6[c]	CH	Al	3.96	8	12.5	1.1[c]
8[d]	DW	NEG	7.5	4	7.25	16.7[d]
10	IVU	Cu	3.64	3.8	3.9	2.9
11	IVU	Cu	4.2	2.5	3.3	3.8
12	IVU	Cu	3.47	4	5.7	1
16	IVU	Cu	3.75	4	3.1	6.6
17	IVU1	Cu	2.13	3	3.4	2.0
17	IVU2	Cu	2.13	3	3.7	1.6
19	IVU	Cu	1.67	2.5	2.8	2.5

Note: [a] Including the contribution from Cells 9,13,15,25,27 and 29, which are identical to Cell 1. [b] Total contribution from all Cells, which have two FCs each. [c] Including the contribution from Cells 14, 20 and 26, which are identical to Cell 6. [d] Including the contribution from Cells 18 and 28, which are identical to Cell 8.

3.1. *Eigenvalue Analysis*

The arbitrary multibunch configuration is defined by M equidistant bunches with N_m particles ($m = 0, .., M-1$), circulating in the storage ring and satisfying the condition $M \leq h$, where h is the number of rf-buckets, with the reference particles of the bunches separated by the distance $d = C/M$, where C is the ring circumference. The eigenvalue equation determining the transverse stability of the multibunch configuration is given by Eq.(46) of[1]

$$(\mathbf{B} - \Omega\mathbf{I})\mathbf{a} = 0, \qquad B_{\mu\mu'} = \frac{\Omega_\mu^U}{NM} \sum_{m=0}^{M-1} N_m e^{i2\pi m(\mu'-\mu)/M}, \tag{6}$$

where $\mathbf{a} = [a_0, .., a_{M-1}]^T$, and Ω_μ^U are the eigenvalues of the uniform filling pattern case ($B_{\mu\mu'} = \Omega_\mu^U$ if $\mu' = \mu$, 0 otherwise), and are given by

$$\Omega_\mu^U = -i\frac{eNMc}{2(E_0/e)T_0^2\omega_\beta} \sum_{p=-\infty}^{+\infty} \left|\tilde{\lambda}\big(pM\omega_0 + \mu\omega_0 + \omega_\beta\big)\right|^2 \bar{Z}_\perp\big[pM\omega_0 + \mu\omega_0 + \omega_\beta\big], \tag{7}$$

where $\sum_{m=0}^{M-1} N_m = NM = N_T$ is the total number of particles in the filling pattern, with N the number of particles per bunch in the uniform filling pattern case, $\omega_0 = 2\pi/T_0$, where T_0 is the revolution period, ω_β is the betatron frequency, e is the electron charge and E_0 is the energy of the reference particle in electron volts. $\tilde{\lambda}(\omega)$ is the Fourier transform of the longitudinal distribution density, assumed to be given and the same for all bunches.

3.2. *Measurements with a Gap in the Uniform Filling*

Measurements of the coupled-bunch instability driven by the vertical resistive wall impedance have been done in the NSLS-II storage ring. with parameters listed in Table 3. The measurements have been performed with the operational lattice at zero linear chromaticity.

Table 3. Parameters for NSLS-II operational lattice.

Parameter	Symbol	Value	Unit
Energy	E_0	3	GeV
Revolution period	T_0	2.64	μs
Harmonic number	h	1320	
Momentum compaction	α	0.00037	
Synchrotron tune	ν_s	0.007	
Horizontal tune	ν_x	33.22	
Vertical tune	ν_y	16.26	
Transverse damping time	$\tau_{x,y}$	22.5	ms
Longitudinal damping time	τ_s	11.9	ms
Energy spread	σ_δ	0.00087	
Bunch length	σ_t	18	ps

Three different multibunch configurations have been studied, as shown in Fig.2, consisting of bunch trains filling the first $M_g = h - g$ rf-buckets, where $h = 1320$ is the harmonic number and g is the gap in the uniform filling pattern. The rectangles in blue, green and red color represent bunch trains with $g = 220$, $g = 920$ and $g = 1220$ respectively. The instability thresholds from measurements are determined from the stability of Beam Position Monitor (BPM) Turn-by-Turn (TbT) data, as discussed in Fig.3, where the three bunch trains with different gaps g are showns at two bunch currents: a stable current, sligthly below threshold (left frame), and an unstable current, sligthly above threshold (rigth frame). The measured instability thresholds, with value between the stable and unstable currents, are compared in Fig.4 with the numerical solution of the eigenvalue equation Eq.(7). The good agreement between theory and simulations, besides benchmarking the eigenanalysis for arbitrary fillings, validates the accuracy of the impedance model used. Additional studies are planned to further corroborate both the theory and impedance model.

References

1. G. Bassi, A. Blednykh and V. Smaluk, Self-consistent simulations and analysis of the coupled-bunch instability for arbitrary multibunch configurations, *Phys. Rev. Acc. and Beams* **39**, 024401 (2016)
2. Brookhaven National Laboratory, 2006, NSLS-II Conceptual Design Report, `https://www.bnl.gov/nsls2/project/CDR/Cover.pdf`.
3. R. D. Kohaupt. DESY-85-139, DESY, Hamburg, Germany (1985).
4. J. S. Berg. Ph.D. thesis, Stanford University, 1996. SLAC-R-478.
5. S. Prabhakar, New diagnostic and cures for coupled-bunch instabilities , SLAC-R-554 (2000); S. Prabhakar, J. D. Fox, and D. Teytelman, Curing Coupled-Bunch Instabilities with Uneven Fills *Phys. Rev. Lett.* **86**, 2022 (2001).

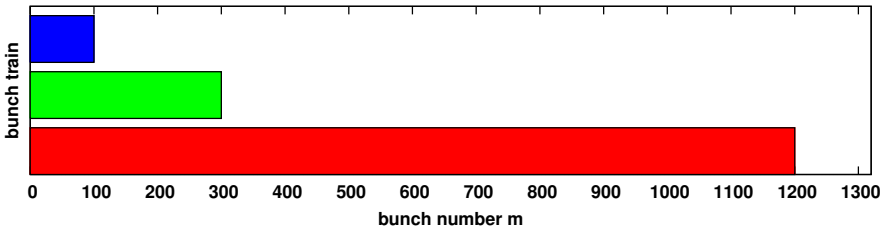

Fig. 2. Bunch trains filling the first $M_g = h - g$ rf-buckets, where h is the harmonic number and g is the gap in the uniform filling pattern. The rectangles in blue, green and red color represent bunch trains with $g = 220$, $g = 920$ and $g = 1220$ respectively.

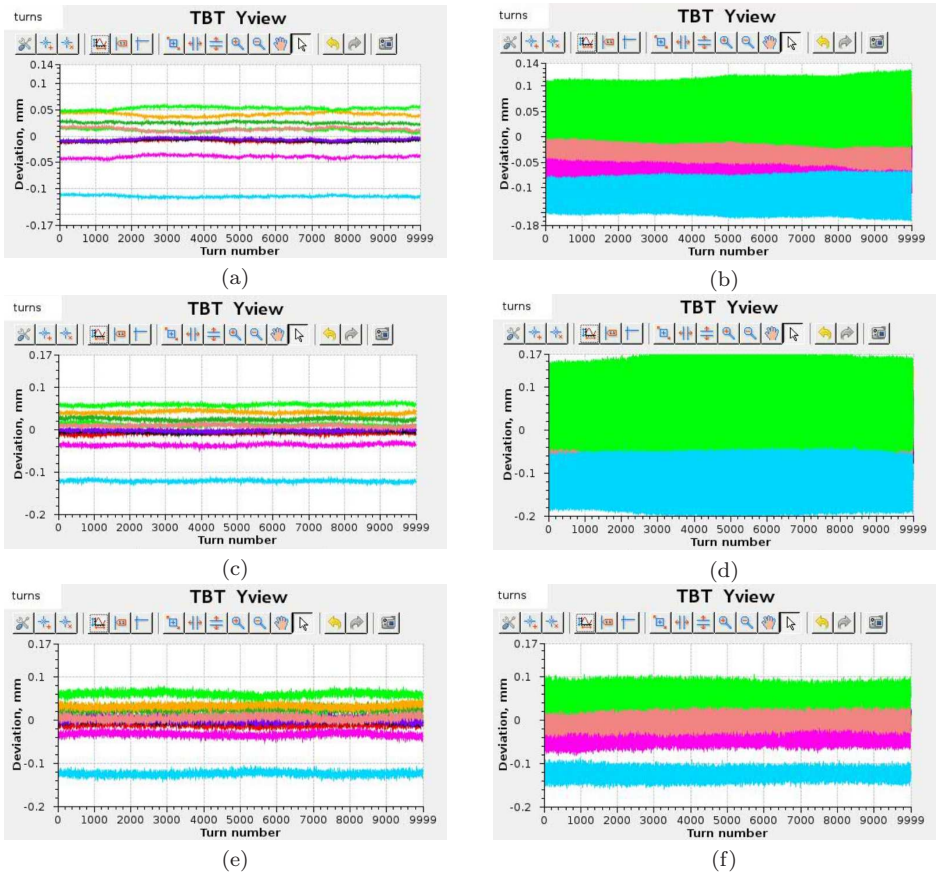

Fig. 3. Snapshots of vertical TbT BPM data (different colors corresponding to different BPMs) taken during measurements of the resistive wall instability threshold for multibunch configurations with three different gaps g, with the left and right frames showing TbT data sligthly below and above threshold respectively. From top to bottom, the gaps and average currents are: $g = 120$, (a) $I_{av} = 10.2$mA and (b) $I_{av} = 11.5$mA; $g = 1020$, (c) $I_{av} = 6.4$mA and (d) $I_{av} = 7.4$mA; $g = 1220$, (e) $I_{av} = 4.0$mA and (f) $I_{av} = 4.7$mA.

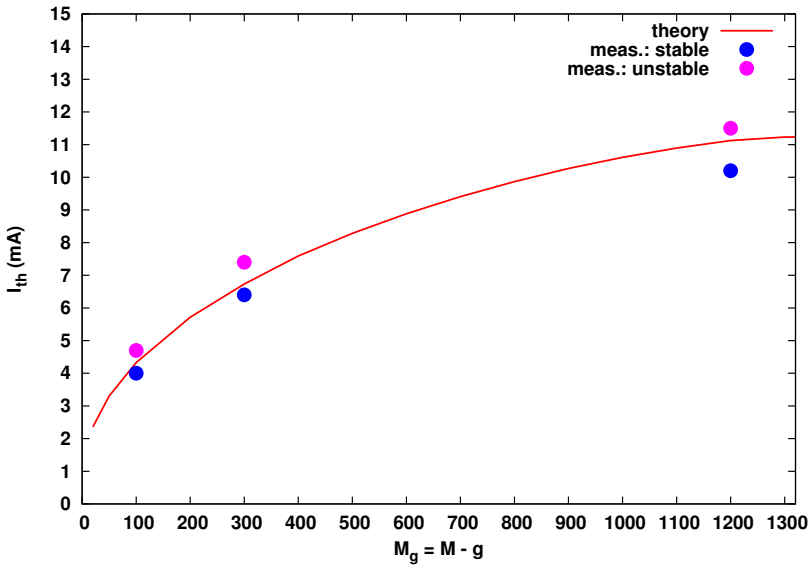

Fig. 4. Coupled-bunch instability threshold as a function of $M_g = h - g$, where g is the gap in the uniform filling pattern. The red line shows the analytical result obtained by equating the fastest growth time (determined by the eigenvalue with the largest imaginary part), the blue and magenta dots represent the measurements slightly below and above threshold respectively.